

Function parametrization: a fast inverse mapping method

B.Ph. van Milligen and N.J. Lopes Cardozo

*FOM Instituut voor Plasma Fysica 'Rijnhuizen', Association EURATOM-FOM,
P.O.Box 1207, 3430 BE Nieuwegein, The Netherlands*

Abstract

Function Parametrization (FP) is a method to invert computer models that map physical parameters describing the state of a physical system onto measurements. It finds a mapping of the measurements onto the physical parameters that requires little computing time to evaluate. The major advantages of FP over other analysis methods are: it is quite general; it is fast, allowing real-time control of experiments; it allows a thorough error analysis; it can provide insight into the structure of the computer program used to model the experiment; it can be used to analyze sets of dissimilar measurements; it can be used to study the adequacy of certain new measurements for determination of specific physical parameters.

FP is tested on the reconstruction of plasma equilibria from magnetic measurements. As a result, some important parameters describing the plasma state are shown to be recoverable in a fast and reliable manner.

1. Introduction

In many experimental situations, the physicist is faced with the problem of interpreting a set of measurements which are implicitly related to the physical parameters of the system under study. In many cases, a model is available that allows explicit simulation of measurements given the physical state of the experiment: the model is a mapping of physical parameters onto measurements. The problem of data interpretation is to find the inverse of the mapping.

However, if the model is complex, this inverse mapping may be hard or impossible to find, or it may not even exist. If a computer model of the experiment is available, the experimenter involved in the interpretation of a set of measurements is then forced to run the model many times, each time adjusting the physical parameters until suitable agreement with his measurements is obtained. If the number of experiments to be done is large, then this iterative solution may become very time-consuming to the point of hindering further advances of the research.

Function Parametrization (FP) is the name for a collection of techniques that tackle the problem of finding an inverse mapping of a computer model systematically. An important ingredient is the reduction of dimensionality of the measuring space such that redundant information is rejected. This procedure must be carried out with great care in order not to discard significant data. The inverse mapping is determined by analyzing a database of simulated experiments. The result of the effort is a simple mapping of a set of measurements onto the physical parameters of the system.

FP is quite generally applicable to many problems of interpretation in modern-day physics. It allows a fast interpretation of measurements, up to the point of real-time control of the experiment. In addition, it can supply insight into the structure of the computer model describing the experiment by displaying relationships and dependencies between parameters. FP can be used to predict the relevance of a new type of measurement to the determination of a specific (set of) parameter(s) even before the measurement device is built. Finally, FP allows a thorough error analysis to be set up, making a clear distinction between systematic and statistical errors, which may not be straightforward with the iterative solution methods mentioned above.

The method of Function Parametrization was first formulated by H. Wind at CERN [1,2], where it was applied to the problem of track finding. The method was then applied to

equilibrium determination at ASDEX by Braams, Jilge and Lackner [3]. Their work was continued by McCarthy [4].

FP relies primarily on well-known statistical methods and the basic principle has been elucidated briefly in a previous publication [3]. This paper attempts to provide a comprehensive description of the method. New additions presented are: (1) an explanation of the behaviour (exponential decay) of the eigenvalues in principal component analysis; (2) a demonstration of the so-called Latent Root Regression; (3) the rationalization of cutoff criteria determining the dimensionality of the regression; (4) a detailed error analysis method. FP is demonstrated with an application to tokamak plasma physics.

2. Theory of Function Parametrization

2.1 Introduction

We consider the situation where a physical model of an experiment is available that allows computation of measurements if the state of the system is known, but where the model is complex enough such that inversion is difficult or impossible.

The state of the physical system, p , is modelled in terms of a finite set of N_p parameters $(p_1, \dots, p_{N_p}) = \vec{p}$ (Appendix B provides a table of notation). Often physical quantities describing the system are functions of e.g. space, and these quantities need to be represented in a parametric form in this formalism (hence the name 'Function Parametrization'). This necessarily involves a reduction in the number of states representable within the context of the parametric form of the model with respect to the full model. But because we are only occupied with those physical states and measurements that are described by a computer model it is always possible to cover all relevant system states by parametric representations.

The N_q measurements that are made on the physical system in the state p are written as a vector $(q_1, \dots, q_{N_q}) = \vec{q}$. The computer model \vec{M} that allows computation of \vec{q} from \vec{p} can be understood to be a mapping $\vec{q} = \vec{M}(\vec{p})$, which can be non-linear. Within the context of the model this mapping is exact. If the model is to make any physical sense, the computation of \vec{q} should be stable against small variations in \vec{p} . On the other hand, it is obvious that most models should be considered to be essentially projections (the information content of the measurements is less than that of the physical parameters), i.e. two physical states \vec{p} and \vec{p}' , $\vec{p} \neq \vec{p}'$, may map to the same measurement: $\vec{q} = \vec{q}'$. Due to finite measurement accuracy this can be formulated even stronger: two different physical states \vec{p} and \vec{p}' may map to two measurement vectors that are indistinguishable given a certain limited measuring accuracy, $\|\vec{q} - \vec{q}'\| < \delta$ for

some norm. Therefore the inverse mapping of \vec{M} is not single-valued. This situation reflects either a fundamental problem in the modelling procedure or a lack in number or accuracy of the measurement data. The problem can be circumvented by restricting the parametrization of p by means of the choice of \vec{p} , such that the inverse mapping, if found, would be single-valued. Even if this is not possible FP can find an inverse mapping, albeit that some components of \vec{p} will be ill-determined, reflecting the non-single-valuedness of the inverse mapping. It will also be shown in the following how the ill-determinedness of some parameters can be detected. Thus, apart from its practical use as an analysis tool, the method can also be used to obtain rudimentary insight into the structure of the model \vec{M} or even the adequacy of the measurements for the purpose of determining the physical parameters \vec{p} .

The method of Function Parametrization (FP) consists of three steps: (1) a database is constructed containing a large number (N) of simulations $\vec{p} = \vec{p}^\alpha$ ($\alpha = 1, \dots, N$), where \vec{p}^α is chosen to lie in the subspace of \mathbf{R}^{N_p} covering (at least) all actual physical states expected to occur in the real experiment. The model \vec{M} is used to compute the corresponding measurements $\vec{q} = \vec{q}^\alpha = \vec{M}(\vec{p}^\alpha)$. (2) the data base is subjected to a statistical analysis, which yields a mapping $\vec{p} = \vec{F}(\vec{q}) + \vec{\epsilon}$, where $\vec{\epsilon}$ is a small error term. The statistical analysis can be subdivided into two parts: (a) a dimension reduction step yielding $\tilde{q} = \vec{g}(\vec{q})$ and (b) a regression yielding $\vec{p} = \vec{f}(\tilde{q})$. Thus $\vec{F}(\vec{q}) = \vec{f}(\vec{g}(\vec{q}))$. (3) the mapping \vec{F} is used in data analysis to interpret real measurements \vec{q} .

We make a distinction between a reduced set of parameters $\{p_j, j \leq N_{id}\}$, $N_{id} \leq N_p$, that are *sufficient* to identify the state p uniquely, and the remaining parameters $\{p_j, N_{id} < j \leq N_p\}$ that are therefore dependent on $\{p_j, j \leq N_{id}\}$ in the context of the model \vec{M} . Note that we do not exclude the possibility that there may be some hidden dependencies (e.g. through some external constraint) between the $\{p_j, j \leq N_{id}\}$. Generation of the data base involves selecting values for the parameters $\{p_j, j \leq N_{id}\}$, and feeding them to the model \vec{M} which will then yield both $\{p_j, N_{id} < j \leq N_p\}$ and \vec{q} . Appendix A.1 gives some suggestions for parameter selection.

2.2 Dimension reduction

There are two reasons for performing the dimension reduction $\vec{g}(\vec{q})$. Firstly, an attempt to fit the components of \vec{p} with linear, quadratic etc. functions of the raw measurement vector \vec{q} in order to determine the mapping $\vec{p} = \vec{F}(\vec{q}) + \vec{\epsilon}$ is bound to fail if N_q is large. If we take \vec{F} to be a polynomial model of degree k , it needs of the order of $N_q^k/(k!)$ fit coefficients for each physical parameter. The number of model simulations needed to determine these coefficients is

considerably larger. Therefore a method by which the dimensionality of the measuring space can be reduced without discarding essential information is required.

Secondly, the measurements are likely to exhibit mutual (linear) dependencies that would make the regression $\vec{f}(\vec{q})$ unstable. Dimension reduction provides a means to stabilize the regression by removing collinearities.

The well-known method of Principal Component Analysis (PCA) achieves dimension reduction by discarding linear combinations ('principal components') of the measurements that show little variation over the database, assuming that they have little relevance in the prediction of parameter behaviour.

This may in some cases not be the best method, because it may be that important information is concealed in principal components that show little variance (e.g. a physical parameter is proportional to a linear combination of the measurements that is almost, but not quite, constant in the database). Conversely, it may be that little information is contained in components that show a large variance (but are largely uncorrelated to the physical parameters of the problem). If either of these are the case, then Latent Root (LR) analysis may be of use.

2.2.1 Principal Component Analysis

The physical parameters \vec{p} and the measurements \vec{q} are normalized. The normalized vectors are called \bar{p} and \bar{q} :

$$\langle x \rangle_j = \frac{1}{N} \sum_{\alpha} x_j^{\alpha}, \quad \sigma_j^2(x) = \frac{1}{N-1} \sum_{\alpha} (x_j^{\alpha} - \langle x \rangle_j)^2 \quad (2.1a)$$

$$\bar{x}_j^{\alpha} = (x_j^{\alpha} - \langle x \rangle_j) / \sigma_j \quad (j = 1, \dots, N_x; \alpha = 1, \dots, N; x = p, q) \quad (2.1b)$$

Here $\langle x \rangle_j$ is the average value of x_j in the data base, and σ_j its spread (i.e. standard deviation).

The dispersion matrices of p and q are computed from :

$$D_{ij}^x = \frac{1}{N-1} \sum_{\alpha} \bar{x}_i^{\alpha} \bar{x}_j^{\alpha} \quad (i, j = 1, \dots, N_x; \alpha = 1, \dots, N; x = p, q) \quad (2.2)$$

The diagonal of D^x contains the squared standard deviations of the \bar{x}_j^{α} , which were normalized to 1. The off-diagonal elements of D^x are the correlations between the components of \bar{x}_j^{α} . D^x is a real, symmetric, positive definite matrix. The eigenvalues of D^x are sorted such that $\lambda_1^x \geq \lambda_2^x \geq \dots \geq \lambda_{N_x}^x \geq 0$. The corresponding orthogonal eigenvectors $D^x \cdot \vec{e}_j = \lambda_j^x \vec{e}_j$ are normalized, $|\vec{e}_j| = 1$.

We define new 'transformed' variables

$$\tilde{x}_j^\alpha = \vec{e}_j \cdot \bar{x}^\alpha. \quad (j = 1, \dots, N_x; \alpha = 1, \dots, N; x = p, q) \quad (2.3)$$

Thus, the components \tilde{x}_j^α of \tilde{x}^α are linear combinations of the \bar{x}_j^α . They have a standard deviation of $\sqrt{\lambda_j}$, and are uncorrelated within the data base. In the following, we shall omit the index α .

By inspection of the eigenvalues, some important remarks can be made about the model \vec{M} . If \vec{M} is a purely linear model, then for $x = p, q$ all λ_j^x for $j > N_{id}$ are equal to 0. In any model, if a component of \vec{x} is linearly dependent on one or more of the independent components of \vec{x} , then the variance of the dependent component is accordingly reduced and the linearly dependent part of its variance is added to the variance of the independent components.

This is an important observation and we shall now illustrate it with a simple example. Suppose we have two measurements \bar{q}_1 and \bar{q}_2 , both normalized in the sense of Eq. 2.1, i.e. $\sigma(\bar{q}_1) = \sigma(\bar{q}_2) = 1$. Suppose that \bar{q}_2 is of the form

$$\bar{q}_2 = \bar{q}_2^i + \beta \bar{q}_1, \quad (2.4)$$

where \bar{q}_2^i is linearly independent of \bar{q}_1 and β is the covariance between \bar{q}_1 and \bar{q}_2 . Then $\sigma^2(\bar{q}_2^i) = 1 - \beta^2$. Computing the dispersion matrix yields:

$$D^q = \begin{pmatrix} 1 & \beta \\ \beta & 1 \end{pmatrix} \quad (2.5)$$

Eigenanalysis yields eigenvalues $\lambda_1 = 1 + \beta$ and $\lambda_2 = 1 - \beta$, and eigenvectors

$$\vec{e}_1 = \frac{1}{\sqrt{2}} \begin{pmatrix} 1 \\ 1 \end{pmatrix} \quad \vec{e}_2 = \frac{1}{\sqrt{2}} \begin{pmatrix} 1 \\ -1 \end{pmatrix}, \quad (2.6)$$

such that, according to Eq. 2.3, $\tilde{q}_1 = (\bar{q}_1 + \bar{q}_2)/\sqrt{2}$ and $\tilde{q}_2 = (\bar{q}_1 - \bar{q}_2)/\sqrt{2}$. Using these expressions to compute the variance of \tilde{q}_1 and \tilde{q}_2 we find $\sigma^2(\tilde{q}_1) = 1 + \beta = \lambda_1$ and $\sigma^2(\tilde{q}_2) = 1 - \beta = \lambda_2$. The covariance becomes $\text{cov}(\tilde{q}_1, \tilde{q}_2) = (N-1)^{-1} \sum \tilde{q}_1 \tilde{q}_2 = 0$, as required. This example clearly demonstrates how the variance $\sigma^2(\tilde{q}_1)$ is incremented by β and the variance $\sigma^2(\tilde{q}_2)$ decremented by the same amount (with respect to $\sigma^2(\bar{q}_1)$ and $\sigma^2(\bar{q}_2)$, respectively) due to the dependency of \bar{q}_2 on \bar{q}_1 given by $\text{cov}(\bar{q}_1, \bar{q}_2) = \beta$.

Now suppose we have not two, but N_q measurements. Suppose the measurements have mutual linear dependencies given by:

$$\bar{q}_1 = \bar{q}_1^i, \quad \bar{q}_2 = \bar{q}_2^i + \beta \bar{q}_1^i, \quad \bar{q}_3 = \bar{q}_3^i + \beta \bar{q}_2^i + \beta \bar{q}_1^i, \text{ etc.} \quad (2.7)$$

Assume $\beta \ll 1$. Thus $\text{cov}(\bar{q}_i, \bar{q}_j) \approx \beta$ ($i \neq j$). This is a fictional set of measurements in which all measurements are equivalent; they all contain an amount of linearly independent information (\bar{q}_i^i)

and they all suffer the same amount of collinearity (β) with all other measurements. By analogy with the preceding example, the \tilde{q}_i have standard deviations given by

$$\sigma^2(\tilde{q}_i) = 1 + (N_q - i)\beta - (i-1)\beta = 1 + \beta(N_q - 2i + 1) \quad (2.8)$$

This implies, for β small,

$$\frac{\sigma^2(\tilde{q}_i)}{\sigma^2(\tilde{q}_{i-1})} = \frac{\lambda_i}{\lambda_{i-1}} = 1 - 2\beta, \quad \text{or } \lambda_i = (1 - 2\beta)^{i-1} \lambda_1 \quad (2.9)$$

It follows that $\lambda_i/\lambda_1 = e^{(i-1) \ln(1-2\beta)}$ (exponential decay of the eigenvalues).

From the fact that the dispersion matrix is computed from the normalized vectors \bar{x} it follows that if \vec{x} shows any linear dependencies between its components at all, $\lambda_1^x > 1$. In an almost purely linear model, where $N_{ld} \approx N_x - N_{id}$ is the number of components of \vec{x} linearly dependent on the minimum set of N_{id} state parameters, the λ_j^x will exponentially decrease in amplitude until $j = N_x - N_{id}$, when they fall to zero sharply. In a model with complicated as well as linear dependencies (as in the second example above), the λ_j^x fall to zero with j approximately exponentially. The steepness of decay depends on the amount of collinearity between the components of \bar{x} (in the example above: small collinearity means β small, so the decay is slow). We introduce a collinearity parameter β_{coll} , given by

$$\ln(1 - 2\beta_{coll}) = -\frac{\partial \ln \lambda_i}{\partial i}. \quad (2.10)$$

The more non-linear the model, the slower the decay and the closer β_{coll} comes to 0. Note however that the parameter ranges also influence the decay: if the parameters p_j , $j=1, \dots, N_{id}$ only vary within narrow ranges a linearized model can give a fairly accurate approximation of a more complex model and the decay of eigenvalues will not be slow.

The \tilde{x}_j are called the 'principal components' of the vector \vec{x} . If real measurements are expected to suffer a relative measuring error of ϵ , it is assumed that those principal components which show a variance over the database of $\lambda_j^x < (3\epsilon)^2$ are both unimportant in the regression and difficult to obtain from real measurements, and we discard them. This is equivalent to the statement that the 'signal' of a principal component should be 'significantly above' (i.e. 3ϵ) the noise level ϵ . The remaining \tilde{x}_j , $j = 1, \dots, N_s$ are called 'significant variables'.

2.2.2 Latent Root Analysis

The objective of the Latent Root (LR) analysis [5] is to find those linear combinations of the normalized measurement vector components \bar{q}_j , $j=1, \dots, N_q$ that show least correlation with a

physical parameter p_k within the data base, and eliminate this linear combination from the regression analysis. We introduce an 'observation vector' \bar{s}^k :

$$\bar{s}^k = (\bar{q}_1, \dots, \bar{q}_{N_q}, \bar{p}_k) = \{\bar{q}, \bar{p}_k\} \quad (k = 1, \dots, N_p). \quad (2.11)$$

Note that we have again omitted the superscript α for convenience. For each simulation in the data base, N_p such 'observation vectors' exist, and they contain the value of all simulated measurements and the k^{th} physical parameter. By analogy with Eq. (2.2), we compute the dispersion matrix:

$$E_{ij}^k = \frac{1}{N-1} \sum_{\alpha} \bar{s}_i^{k-\alpha} \bar{s}_j^{k-\alpha} \quad (i, j = 1, \dots, N_q+1) \quad (2.12)$$

The diagonal of E^k again contains the squared standard deviations of the components of \bar{s}^k , which were normalized to 1. The off-diagonal elements are the cross-correlations. Of special interest are the $E_{i(N_q+1)}^k$ elements, the correlations between \bar{p}_k and the measurements.

Analogous to the procedure in Section 2.2.1 the eigenvalues and corresponding eigenvectors of E^k are computed. The eigenvalues λ_j^k are called latent roots and the normalized eigenvectors \bar{r}_j^k are called latent vectors. They satisfy

$$E^k \bar{r}_j^k = \lambda_j^k \bar{r}_j^k, \quad |\bar{r}_j^k| = 1 \quad (2.13)$$

The latent roots and vectors have some interesting properties. For instance, if, for some j , $\lambda_j^k = 0$ while $(\bar{r}_j^k)_{N_q+1} \neq 0$ (where $(\bar{r}_j^k)_{N_q+1}$ is the last component of \bar{r}_j^k) then Eq. (2.13) demonstrates that there exists an exact linear relationship between \bar{p}_k and \bar{q} :

$$\bar{p}_k = - \frac{1}{(\bar{r}_j^k)_{N_q+1}} \sum_{i=1}^{N_q} (\bar{r}_j^k)_i \bar{q}_i \quad (2.14)$$

No regression is necessary as Eq. (2.14) gives a direct relation between measurements and the physical parameter \bar{p}_k . But exact linear relationships are hard to find in reality, of course, and this situation will seldomly occur.

If, for some j , both $\lambda_j = 0$ and $(\bar{r}_j^k)_{N_q+1} = 0$, there exists an exact linear dependence among the measurements. This non-predictive singularity can be removed by discarding the corresponding \tilde{q}_j , where

$$\tilde{q}_j = \sum_{i=1}^{N_q} (\bar{r}_j^k)_i \bar{q}_i \quad (2.15)$$

Again this ideal singularity with exact linear relationships between the measurements will hardly ever occur in reality, but there may very well be near-singularities with $\lambda_j < \gamma$ and $(\bar{r}_j^k)_{N_q+1} < \delta$, where γ and δ are small numbers. The same discarding procedure can be applied once the discriminatory levels γ and δ are set.

The improvement upon the simple PCA procedure is obvious: linear combinations of the measurements that show large variance in the database but have little or no correlation to the physical parameters would have been included in the regression following PCA, but can now be detected and discarded. A disadvantage is that the computing time required both for determining the mapping \vec{F} and its evaluation for real measurements takes considerably more time than the PCA procedure.

2.3 Regression

In order to obtain the mapping \vec{F} , we perform a regression of p_j in terms of functions of \tilde{q}_k for each j . We remark that it is also possible to regress \tilde{p}_j , rather than p_j , but the reduction in dimensionality of the fitting problem thus obtained generally does not compensate for the increase in complexity of the results. We demonstrate the procedure with a simple polynomial fit, which takes the form

$$p_j = c_{j0}\phi_0 + \sum_{k=0}^{N_1} c_{j1}^k \phi_1 \left[\frac{\tilde{q}_k}{\tilde{\sigma}_k} \right] + \sum_{k=0}^{N_2} \sum_{l=k+1}^{N_2} c_{j2}^{kl} \phi_1 \left[\frac{\tilde{q}_k}{\tilde{\sigma}_k} \right] \phi_1 \left[\frac{\tilde{q}_l}{\tilde{\sigma}_l} \right] + \sum_{k=0}^{N_2} c_{j2}^{kk} \phi_2 \left[\frac{\tilde{q}_k}{\tilde{\sigma}_k} \right] + \dots + \epsilon_j, \quad (2.16)$$

where $N_n \leq N_s$, the ϕ_n are suitable polynomials of the n^{th} degree, $\tilde{\sigma}_j = \sqrt{\lambda_j}$ and the c 's are the regression coefficients. The multi-dimensional polynomial functions are referred to as 'basis functions'. N_1 is the number of \tilde{q}_i used in constructing linear basis functions, N_2 the number used in constructing quadratic basis functions, etc. The N_n 's can be chosen equal to N_s for all n , but generally results are more stable with respect to measurement noise if only $N_1 \approx N_s$, and the higher-order N_n 's are taken smaller. It is actually possible to use stability with respect to measurement noise as a selection criterion for N_n . We shall demonstrate this in Section 3.4. It is now possible to write Eq. (2.16) as a simple sum over fit coefficients multiplied by basis functions, which demonstrates that even for non-linear models the regression problem is linear.

We have normalized the significant components to their standard deviations $\tilde{\sigma}_j = \sqrt{\lambda_j}$ (where we have omitted the superscript q) such that the arguments of the polynomials ϕ_n are normalized. This normalization is not strictly necessary. The $\tilde{q}_i/\tilde{\sigma}_i$ are linearly independent: $\text{cov}(\tilde{q}_i/\tilde{\sigma}_i, \tilde{q}_j/\tilde{\sigma}_j) = \delta_{ij}$, where δ_{ij} is the Kronecker symbol. However, the $\phi_n(\tilde{q}_i/\tilde{\sigma}_i)$ should also be linearly independent for all n and i in order for the regression to be well-determined. The Hermite polynomials H_n satisfy this requirement because, if $\phi_n = H_n$, $\text{cov}(\phi_n(y), \phi_m(y)) = \delta_{nm}$ if y is a random variable with a normal probability distribution, which makes them well-suited to our purpose.

From Eq. (2.16) one may deduce that the total number of basis functions, N_{bf} is given by:

$$N_{\text{bf}} = \sum_{n=0}^{N_{\text{or}}} \frac{(N_n + n - 1)!}{n! (N_n - 1)!}, \quad (2.17)$$

where $N_0 \equiv 1$ and N_{or} is the order of the fitting polynomial (2.16). The N_n 's must be chosen such that $N_{\text{bf}} < N$ to prevent the regression from being underdetermined, and preferably $N_{\text{bf}} \ll N$.

The regression is performed, and the fitting coefficients c in Eq. (2.16) are found. The regression is an ordinary linear least-squares regression. Some caution in carrying out this regression is necessary, because although the principal components are linearly independent, the basis functions that are constructed from them may show small collinearity. But if small collinearity is present, the fitting coefficients c may take on huge meaningless values that do not show up when checking the result of the regression on the unperturbed measurements in the database (see Section 2.4), but can seriously influence the interpretation of real measurements. Therefore, the significant variables should be perturbed with small random variations ϵ_{pre} prior to the regression so as to destroy this remaining collinearity completely, while leaving all significant information intact. The amplitude of ϵ_{pre} is not critical as long as it is small: $\epsilon_{\text{pre}} \approx \epsilon/3$ is a safe choice (where ϵ is the typical relative measurement error). Other methods of regularization of the regression might also be used.

Thus, we finally have obtained the mapping \vec{F} , which is given in terms of the averages and standard deviations of \vec{q} in the database, the eigenvectors and eigenvalues of D^q , the choice and number of basis functions, and the fitting coefficients c .

2.4 Error Analysis

The systematic error in the reconstruction of physical parameters by means of the method described above is due to several distinct sources: (1a) the (analytical) model itself is only an approximation of the physical system and the simulated measurements do not contain as much information as the physical quantities in the model, (1b) the parametrization of the model (i.e. the computer model) is a further limitation in the description that may lead to errors, (1c) the dimension reduction as described in Section 2.2 reduces information content of the measurements, and (1d) the regression, being a least-squares fit, reduces the information content even further. The statistical error in the reconstruction is due to (2a) measurement errors, (2b) digitizing noise in the measurements, and (2c) computational inaccuracy in the evaluation of \vec{F} . In the following, we indicate how the combined effect of these systematic (except for (1a)) and statistical errors can be estimated. Note that random measurement noise having a normal (Gaussian) distribution may lead to skew statistical errors in the physical parameters. We do not investigate this here, but it is easy to evaluate this skewness numerically using the mapping \vec{F} .

2.4.1 Definition of error measures

We study the reliability and sensitivity to measurement noise of the mapping \vec{F} found in Section 2.3. The systematic error introduced by the mapping can be estimated by computing the physical parameters from the simulated data in the database using the mapping \vec{F} and comparing them to the stored values p_j . The systematic reconstruction error is defined as

$$(\epsilon_j^{\text{sys}})^2 = \frac{1}{N-1} \sum_{\alpha} (F_j(\vec{q}_{\alpha}) - p_{j\alpha})^2, \quad (2.18)$$

where α runs over all N simulations. ϵ_j^{sys} is the average systematic error over the data base of the j^{th} parameter.

The statistical error in the computation of p_j can be estimated for any observation \vec{q} individually by

$$(\epsilon_j^{\text{stat}})^2 = \frac{1}{N_{\text{stat}}-1} \sum_{\beta} (F_j(\vec{q} + \vec{\epsilon}_{\beta}) - F_j(\vec{q}))^2, \quad (2.19)$$

where β runs from 1 to N_{stat} (chosen arbitrarily but not too small) and $\vec{\epsilon}_{\beta}$ is a vector of random variables. The standard deviation of the i^{th} component of $\vec{\epsilon}_{\beta}$, $\sigma(\epsilon_{\beta i})$, is equal to the measurement error in the i^{th} measurement. ϵ_j^{stat} is a function of \vec{q} and therefore variable over the data base. We compute ϵ_j^{stat} at the centre of the data base parameter space. Nevertheless the

statistical error can also be evaluated for real measurement data, giving a precise measure for the noise contribution in the reconstruction error.

The combined effect of the statistical and systematic error, the total reconstruction error, containing the effects of both the systematical and the statistical error can be estimated from

$$(\epsilon_j^{\text{rec}})^2 = \frac{1}{N-1} \sum_{\alpha} (F_j(\vec{q}_{\alpha} + \vec{\epsilon}_{\alpha}) - p_{j\alpha})^2, \quad (2.20)$$

where α runs from 1 to N . Approximately, $(\epsilon_j^{\text{rec}})^2 \approx (\epsilon_j^{\text{sys}})^2 + (\epsilon_j^{\text{stat}})^2$.

If the spread of a parameter within the database is small, the error ϵ_j may also be small without predicting variations in the parameter correctly. Therefore the quantity ϵ_j/σ_j is considered a better indicator for the quality of parameter reconstruction than ϵ_j itself.

The error estimates (2.18) and (2.20) allow us to search for an optimal combination of basis functions that gives maximum reconstruction accuracy while being not too sensitive to measurement noise.

2.4.2 Reconstruction qualifier

The results obtained by FP are only valid for physical states within, or close to, the subspace of the total physical state space covered by the data base. If a physical state lies within this subspace, we know that the quality of the reconstruction can be estimated by means of the error measures defined in the previous Section. A measure for the reliability of the results is therefore:

$$Q = \frac{1}{N_q} \sum_{i=1}^{N_q} \frac{\tilde{q}^2(i)}{\lambda_i + (\tilde{\epsilon}_i^{\text{meas}})^2}, \quad (2.21)$$

where $\tilde{\epsilon}_i^{\text{meas}}$ is the relative error that the transformed measurement i suffers due to the measurement errors $\{\epsilon_i^{\text{meas}}, i=1, \dots, N_q\}$. Thus, Q is an indicator for "closeness" of a measurement to the "centre" of the subspace (of the total parameter space) that is covered by the simulations. If $Q \approx 1$, the measurement is well represented within the database and the accuracy estimates made above apply. If $Q \gg 1$ ($Q > 4$) for a particular measurement, the results obtained by FP are extrapolations beyond the boundaries of the simulated subspace and no indication of the accuracy can be given. Such an observation can be ignored, or, if it is known that the measurements are not at fault, the data base can be extended to include the experimental situations not covered in the existing database, or, if it is known that one or more specific measurement signals are failing, these can be reconstructed by minimizing (2.21) while keeping the correct signals fixed.

3. Application to the RTP tokamak

3.1 Introduction

3.1.1 Tokamak physics

We shall illustrate the procedure of FP with an example from tokamak plasma physics. A tokamak plasma is a toroidally shaped ionized gas through which a large current flows in the toroidal (ϕ) direction, along the externally imposed toroidal magnetic field (the geometry is clarified in Fig. 3.1). The current produces a magnetic field in the poloidal (transverse) direction which balances the outward $-\nabla p$ pressure gradient force by an inward $\vec{j} \times \vec{B}$ force (\vec{j} is the current density). When these forces are equal and opposite, the plasma is in equilibrium. Treating the plasma as a single-species ideally conducting fluid and assuming toroidal rotational invariance, the equations governing the equilibrium (the pressure balance supplemented with the Maxwell equations), can be written down in terms of the poloidal flux function ψ . The poloidal magnetic field is given by

$$\vec{B}_p = -\frac{1}{R} \nabla \psi \times \vec{e}_\phi, \quad (3.1)$$

where we have adopted the usual cylindrical coordinate system (R, Z, ϕ) . The equilibrium equation can be written

$$\Delta^* \psi = \left[R \frac{\partial}{\partial R} \frac{1}{R} \frac{\partial}{\partial R} + \frac{\partial^2}{\partial Z^2} \right] \psi = -\mu_0 R j_\phi = -\mu_0 R^2 p' - FF', \quad (3.2)$$

where j_ϕ is the toroidal current density, $p(\psi)$ is the pressure, $F(\psi) = RB_\phi$ which is related to the poloidal current density and ' denotes $\partial/\partial\psi$. This is known as the Grad-Shafranov (GS) equation [6]. It is a second-order differential equation with 2 source functions (p and F). If the source functions and suitable boundary conditions are given, a single solution $\psi(R, Z)$ can be found by solving the equation. In an experimental situation, however, the source functions are not known *a priori*.

3.1.2 RTP

The Rijnhuizen Tokamak Project (RTP) Tokamak is schematically shown in Fig. 3.1. The experimental data consist of 12 poloidal field measurements (made at the locations indicated by 'pickup coils' in Fig. 3.1), 12 radial field measurements (made using wire loops attached to the liner) and a measurement of the toroidal field B_0 , so $N_q = 25$. The physical parameters of

interest are, e.g., the location of the plasma boundary or the current density at the plasma centre.

Given the kind of measurements available, solution of the GS equation is only possible by making restrictive assumptions with regard to the source functions in Eq. (3.2) (generally referred to as 'profiles'). Even then the solution procedure is time-consuming: it consists of selecting the two profiles, solving the equilibrium, computing the corresponding magnetic data and iteratively adjusting the profiles and other parameters until a satisfactory reproduction of the real measurements is found. This procedure has to be carried out $O(100)$ times for a single experiment lasting 100 ms in order to get an indication of the time-development of the plasma, and several tens of experiments can be carried out each day. This leads to an intolerable burden on the computer system with traditional equilibrium solver programs. FP provides the means to make such analysis feasible.

3.2 Parametrization

In our example the reduced set of parameters $\{p_j, j \leq N_{id}\}$ used in identifying the equilibrium are the following. (1) I_p is the total current flowing through the plasma. (2) B_0 is the value of the toroidal field on the torus axis. (3,4) (R_{geo}, Z_{geo}) is the location of the geometrical centre of the plasma boundary in cylindrical coordinates. (5) a_{min} is the minor radius of the plasma. We have assumed the plasma to have a circular shape in a poloidal cross-section, and the flux surfaces are taken to be circular as well. The plasma column is assumed to have up-down symmetry with regard to the $Z = Z_{geo}$ plane. (6) δ is the 'Shafranov shift', i.e. the outward displacement of the magnetic axis with respect to R_{geo} ($\delta = \Delta/a_{min}$, where Δ is the Shafranov shift in m, see Fig. 3.1). δ is closely related to the central pressure. (7,8,9,10) The remaining quantities are profile parameters ($a_\Gamma, e_\Gamma, a_\Pi, e_\Pi$, explained below). Thus, $N_{id} = 10$.

The profiles are written down in a dimensionless form (unit profiles). The amplitude of the profiles is then given by the other parameters, and the unit profiles themselves only contain shape information. The unit profiles are chosen to be:

$$\Gamma(\psi) = (1 + a_\Gamma\psi + b_\Gamma\psi^2)^{e_\Gamma} \quad (a_\Gamma + b_\Gamma = -1) \quad (3.3a)$$

$$\Pi(\psi) = (1 + a_\Pi\psi + b_\Pi\psi^2)^{e_\Pi} \quad (a_\Pi + b_\Pi = -1) \quad (3.3b)$$

Here ψ is a normalized flux coordinate: $\psi = 0$ on axis and $\psi = 1$ at the plasma boundary. This choice of profile parametrization is motivated by the observation that measurements made on typical RTP discharges can be well reproduced by equilibria generated using this parametrization. The unit profiles Γ and Π , appearing in the HBT equilibrium solver [7], are

related to the pressure derivative (p') and poloidal current (FF') profiles mentioned above through:

$$p'(\psi) = -\frac{AB\epsilon B_0^2}{2\alpha^2} \Pi(\psi) \quad (3.4a)$$

$$FF'(\psi) = \frac{a_{\min}^2 AB_0^2}{\alpha^2} \left[\Gamma(\psi) - \frac{B}{2\epsilon} \Pi(\psi) \right] \quad (3.4b)$$

where A and B are eigenvalues of the GS equation and α is a dimensionless parameter measuring the total poloidal flux: $\alpha = a_{\min}^2 B_0 / \Phi_1$ (here Φ_1 is the unnormalized flux at the plasma boundary). A, B, α and Φ_1 are determined by the MHD equilibrium code HBT.

Table A.1 (Appendix) lists the values of the parameter ranges used for the creation of a database covering the RTP experiment ($N = 1000$ simulations). The central value was found by analyzing a typical discharge (R19900321.017) at $t=50$ ms. (in the so-called flat-top or steady-state phase). We defined a χ^2 :

$$\chi^2 = \sum_{N_q} \frac{(q_i - q_i^{\text{meas}})^2}{(\epsilon_i^{\text{meas}})^2} \quad (3.5)$$

Where ϵ_i^{meas} is the measurement error in the i^{th} measurement q_i^{meas} . We then computed an equilibrium with arbitrary choice of the parameter values and computed χ^2 from the simulated measurements q_i . We chose slightly different values of the parameters and iterated, thus minimizing χ^2 until it reached a value close to N_q , indicating good reproduction of the measurements. This equilibrium was taken as central value for the database. Note that the profiles used are fairly broad, reflecting the current type of plasmas produced in the experiment. In the near future, more peaked profiles might become more common. Should the need for such a change in parametrization occur, the reconstruction qualifier Q discussed in Section 2.4.2 will automatically signal this and a new database using e.g. narrower profiles can be constructed.

3.3 Principal Component Analysis

We performed PCA exactly along the lines of Section 2.2.1. First we determined the eigenvalues of the dispersion matrix of \vec{q} . Fig. 3.2 displays the eigenvalues vs. their index numebr graphically. As expected, they decay exponentially (cf. Eq. (2.9)). If we determine β_{coll} (Eq. (2.10)) from the exponential decay, ignoring the non-exponential tail for $i > 20$ that is due to finite computational accuracy, it follows: $\beta_{\text{coll}}(\text{RTP}) = 0.29$.

The second step in PCA is the discarding of principal components. The relative measurement error in the magnetic measurements at RTP is approximately 3%. This suggests (cf. Section 2.2.1) a cutoff at $\lambda = (3 \cdot 0.03)^2$ which we have marked in Fig. 3.2. Thus, keeping only 9 of the 25 principal components might already be sufficient to reproduce the plasma parameters within measuring accuracy. We will investigate this further in Section 3.4.

3.4 Regression and error analysis

3.4.1 Regression based on PCA

Table 3.1 lists the error estimates defined in Section 2.4.1 for the RTP database. We have performed the regression along the lines of Section 2.3, using the polynomial regression model with Hermite polynomials.

Table 3.1: Plasma parameter reconstruction error analysis for RTP database
 $N_1 = 8, N_2 = 3$. (σ 's and ϵ 's normalized to the central value)

Parameter	I_p	R_{geo}	a_{min}	δ
Central value	100000.	0.721	0.133	0.0617
Spread, σ_j	0.22	0.048	0.13	0.13
ϵ_j^{sys}	0.0022	0.0039	0.062	0.12
ϵ_j^{stat}	0.0093	0.0019	0.014	0.011
ϵ_j^{rec}	0.0093	0.0043	0.064	0.12
$\epsilon_j^{\text{sys}}/\sigma_j$ (%)	0.96	8.0	47.	93.
$\epsilon_j^{\text{stat}}/\sigma_j$ (%)	4.2	4.0	11.	8.5
$\epsilon_j^{\text{rec}}/\sigma_j$ (%)	4.2	8.9	48.	94.

Table 3.1 clearly demonstrates how some parameters are easily recovered from the magnetic data while others are hard to determine at all. The reconstruction of I_p (which can analytically be expressed as a simple sum over the poloidal field measurements) is dominated by the statistical error. The other parameters listed here have reconstruction errors that are dominated by the systematical error.

Of course, many more parameters than the ones listed in Table 3.1 are available to describe the plasma state p . Tables like 3.1 can also be used to determine which plasma

parameters can be determined most accurately from the available measurements and are therefore best suited for the purpose of giving a description of the plasma. In this manner we have found that of the two most common sets of moments used in describing the magnetic field outside the plasma, i.e. current and multipole moments [8], current moments are best by far.

The error estimates (2.18) and (2.20) allow us to search for an optimal combination of basis functions giving maximum reconstruction accuracy while being not too sensitive to measurement noise. The data in Table 3.1 were compiled from a reconstruction that was already optimized. We shall now demonstrate how we came to this choice of basis functions.

While ϵ_j^{sys} decreases monotonically with the number of basis functions, ϵ_j^{stat} increases, leading to an optimum (i.e. minimum) in ϵ_j^{rec} . Taking too many basis functions deteriorates the regression results, because the higher-order basis functions are more sensitive to noise.

Figures 3.3, 3.4 and 3.5 illustrate the behaviour of ϵ_j^{sys} and ϵ_j^{rec} as a function of the amount of linear and quadratic basis functions (N_1 and N_2 , respectively, see Eq. (2.8)). We have selected a_{min} and R_{geo} as illustrations of the procedure. From Fig. 3.2 we expect the reconstruction to be optimal at $N_1 = 9$ in Fig. 3.3. In fact, what we see is that the first 5 principal components already contain the essential information necessary for reconstruction of a_{min} . The predicted minimum in ϵ_j^{rec} is fairly broad (from $N_1 = 5$ to 10), and taking N_1 anywhere in this range will not influence the reconstruction significantly. Note that taking $N_1 = 11$ ($= N_{\text{id}}+1$!) or more leads to a significant reduction of ϵ_j^{sys} but unacceptable instability with respect to measurement noise. We selected $N_1 = 8$ on the basis of graphs like Fig. 3.3 for other parameters, keeping in mind that N_1 should be equal to N_{id} , approximately. Having selected N_1 , we proceeded along similar lines for the selection on N_2 (Fig. 3.4). N_2 does not have a significant influence on the reconstruction of a_{min} as long as $N_2 \leq 6$, but it does on the reconstruction of R_{geo} (Fig. 3.5). Also, the computing time is a strong function of the N_n 's (see Eq. 2.5). This motivated us to select $N_2 = 3$.

3.4.2 Regression based on LR

We have analyzed the same RTP database with the Latent Root analysis method. We found that in order to keep between 6 and 8 principal components, the discriminatory levels γ and δ should be chosen $\gamma = \delta = 0.3$. The actual number of principal components kept is different for each plasma parameter, of course: e.g. accurate reconstruction of the plasma current I_p requires less principal components than any other plasma parameter. This is demonstrated by the listed number of principal components in Table 3.2.

Also listed in Table 3.2 is the reconstruction accuracy for each parameter. The numbers listed should be compared to those of Table 3.1. The Latent Root method in the case studied here reduces the systematical error, while increasing the statistical error slightly. The total reconstruction error ϵ_j^{rec} using LR is slightly better than the one using PCA. For most plasma parameters the difference is only slight, however, except for δ . LR has detected and removed a non-predictive principal component for this parameter.

Table 3.2: Plasma parameter reconstruction error analysis for RTP database using LR. N_1 is equal to the number of principal components kept: N_{prin} , and $N_2 = 6$. (σ 's and ϵ 's normalized to the central value)

Parameter	I_p	R_{geo}	a_{min}	δ
N_{prin}	6	7	7	7
Central value	100000.	0.721	0.133	0.0617
Spread, σ_j	0.22	0.048	0.13	0.13
ϵ_j^{sys}	0.0011	0.0036	0.052	0.085
ϵ_j^{stat}	0.0090	0.0022	0.031	0.035
ϵ_j^{rec}	0.0097	0.0043	0.064	0.098
$\epsilon_j^{\text{sys}}/\sigma_j$ (%)	0.47	7.6	39.	66.
$\epsilon_j^{\text{stat}}/\sigma_j$ (%)	4.0	4.6	23.	27.
$\epsilon_j^{\text{rec}}/\sigma_j$ (%)	4.3	8.9	48.	76.

3.5 Results

Figures 3.6 through 3.9 show the time traces of some plasma parameters that were obtained from real measurements using FP, for RTP discharge R19900321.017.

Figure 3.6 shows the time trace of the plasma current. After initiation of the experiment, it rises quickly to 100 kA, to remain in the 'flat-top' phase for approximately 100 ms.

Figure 3.7a shows the time trace of R_{geo} . Initially, there is a large oscillatory movement that is due to an imperfection in the plasma position control. The FP signal can be compared to the Δ_{hor} signal, which is simply the position of the weighted current centre with respect to the $R = 0.72$ (or central) position. This signal is displayed in Fig. 3.7b, and compares well to 3.7a.

Fig. 3.8 displays the time trace of the a_{\min} signal. During the flat-top phase, it attains the maximum value (0.178 m) dictated by the circular limiter (Fig. 3.1) within measuring accuracy.

Fig. 3.9 displays the reconstruction qualifier Q . Apart from spikes at the beginning, it stays low (≈ 2) during the entire shot, indicating reliable reconstruction.

4. Summary and Conclusions

4.1 Principle and Advantages of Function Parametrization

Function Parametrization is a method to invert computer models that map physical parameters that describe the state of a physical system onto measurements. The method involves generating and storing a large number of well-chosen simulations and statistically analyzing these. The result is a mapping of the measurements onto the physical parameters that requires little computing time to evaluate. The major advantages of FP over other analysis methods are: it is quite general; it is fast, allowing real-time control of experiments; it allows a thorough error analysis (as was demonstrated in this paper); it can provide insight into the structure of the computer program used to model the experiment; it can be used to analyze sets of dissimilar measurements; it can be used to study the adequacy of certain new measurements for determination of specific physical parameters (even before the measuring equipment is built).

4.2 Power and Limitations of Function Parametrization

Generally, the computer model mapping the physical parameters onto the measurements reduces information content, i.e. the measurements do not represent full knowledge of the physical system, or, in other words, the mapping is essentially a projection. This necessarily means the inverse mapping cannot determine all physical parameters exactly. This problem can be circumvented by restricting the physical parameter space, i.e. by choosing a certain parametrization of the physical system that limits the solutions of the inverse problem to a certain class, provided knowledge is available to confidently make this restriction without excluding essential parts of the physical state space. Alternatively, one may decide to accept such ill-determinedness of some physical parameters as being inherent to the analysis of inadequate measurements.

On the other hand, the measurements generally also contain redundant information. As the inverse mapping method relies on regression analysis, large dimensionality of the measurement space and mutual (linear) dependencies between the measurements are undesirable. Two methods are suggested to reduce the dimensionality of the measuring space

without rejecting essential information: Principal Component Analysis (PCA) and Latent Root Analysis (LR).

PCA selects those linear combinations of the measurements that have maximum variance within the database. Generally, these will also have the highest predictive relevance. However, if the computer model is not very stable there may be combinations of the measurements that show a large variance over the data base but have little relevance to the physical parameters. Also, a specific parameter may be related to a subset of the measurements that show only small variance (rather than all measurements). In these cases Latent Root analysis may improve the solution of the model inversion problem, as it selects those combinations of the measurements that have highest correlation with specific physical parameters.

4.3 Application to Tokamak Physics: RTP

The practical example of Tokamak equilibrium reconstruction presented in this paper demonstrates that FP is capable of making a fast, accurate and reliable computation of plasma parameters from the magnetic measurements presently available at the RTP experiment. As soon as other relevant measurements become available (e.g. polarimetry or SXR measurements), these can also be incorporated in the analysis to help determine the equilibrium more accurately, and in more detail. FP has already been successfully applied to polarimetric data at the TEXTOR tokamak [9], and this is anticipated for RTP as well (in combination with magnetic data). Also, FP is fast enough to make it a likely candidate for real-time plasma control and feedback.

4.4 Conclusions

The method of Function Parametrization provides a means to carry out fast data analysis of measurements done on physical systems modelled with large and complex computer codes. The analysis can be carried out using only minimal computing time. This is achieved by concentrating the main computational effort before the beginning of the physical experiment.

The method may be of use in other contexts as well: it may relieve any repetitive running of large computer programs, or at least give a first approximation of the solutions that such programs attempt to find, thus reducing the searching effort. Its use is also indicated with expert systems.

Appendix

A.1 Database generation: Method of parameter selection

Database generation is carried out by selecting the N_{id} independent parameters p_j , $j=1, \dots, N_{\text{id}}$ randomly from a range R_j : $p_j^{\text{min}} \leq p_j \leq p_j^{\text{max}}$, computing the remaining plasma parameters and the measurements, and repeating this N times. The random selection is made using a truncated normal (i.e. Gaussian) probability distribution function $f_j(p_j)$ with its maximum at p_j^{prim} (where $p_j^{\text{min}} \leq p_j^{\text{prim}} \leq p_j^{\text{max}}$) and width σ_j (Fig. A.1). The choice of a Gaussian-type probability distribution function is not essential to the method. The upper and lower boundaries only serve to prevent extremely unlikely states of the plasma to be included in the database. The value of p_j^{prim} is inspired by expectations about the most likely experimental situation as indicated above, and likewise the choice of σ_j is inspired by the expected spread. This procedure will cause the regression (see below) to be most accurate near the most likely experimental situation.

A.2 Database generation (RTP)

Table A.1: Plasma state parameter distribution settings for database generation

Parameter	Lower bound	Central value	Upper bound	Spread, σ
I_p	10000.	100000.	150000.	30000.
B_0	1.0	2.03	2.3	0.2
R_{geo}	0.65	0.72	0.80	0.04
Z_{geo}	-0.05	0.	0.05	0.02
a_{min}	0.09	0.173	0.178	0.04
δ	0.04	0.0555	0.1	0.01
a_{Γ}	-1.2	-1.0	-0.8	0.1
e_{Γ}	0.2	0.7	1.2	0.2
a_{Π}	-1.2	-1.0	-0.8	0.1
e_{Π}	0.1	0.3	0.8	0.15

B Table of notation

p	state of a physical system
\vec{p}	physical parameter vector (p_1, \dots, p_{N_p})
\vec{q}	measurement vector (q_1, \dots, q_{N_q})
\vec{M}	computer model $\vec{q} = \vec{M}(\vec{p})$
\vec{F}	inverse mapping $\vec{p} = \vec{F}(\vec{q}) + \vec{\epsilon}$
N	number of simulations = size of database $(\alpha = 1, \dots, N)$
N_p	number of physical parameters $(j = 1, \dots, N_p)$
N_q	number of measurements $(i = 1, \dots, N_q)$
N_{id}	number of physical parameters sufficient to identify a physical state
$\langle x \rangle_j$	average of x_j
$\sigma_j(x)$	standard deviation of x_j
\bar{x}	normalized vector \vec{x} (i.e. having zero mean and unit standard deviation)
\tilde{x}	'transformed' vector \vec{x} (having linearly independent components in the database)
N_s	number of significant variables
$\phi_n(x)$	basis function of n^{th} order in x
c_{ij}	regression coefficient
N_n	number of 'transformed' vector components used in constructing basis functions of n^{th} order

Acknowledgements

The authors would like to express their gratitude to Bas Braams and Chris Schüller for fruitful discussions on the subject of Function Parametrization. A short collaboration with Patrick McCarthy and Karl Lackner at ASDEX has been inspiring and we are indebted to them for providing much insight into the matter. The idea of Latent Root Analysis and some of the algorithms used in the present work are due to Patrick McCarthy. This work was performed under the Euratom-FOM Association agreement with financial support from NWO and Euratom.

References

- [1] WIND, H.: in CERN Computing and Data Processing School (Proc. 1972 School) CERN 72-21 (1972) 53
- [2] WIND, H.: (a) Principal component analysis and its application to track finding, (b) in *Formulae and Methods in Experimental Data Evaluation*, Vol. 3, European Physical Society, Geneva (1984).
- [3] BRAAMS, B.J., JILGE, W., LACKNER, K., Nucl. Fusion 6 (1986) 699
- [4] MCCARTHY, P.J., SEXTON, M.C., *Plasma profile recovery by function parametrization*, Max-Planck Institut für Plasmaphysik, Report IPP 5/12 (1986)
- [5] WEBSTER, J.T., GUNST, R.F., MASON, R.L.: *Latent Root Regression Analysis*, Technometrics, Vol. 16, No. 4 (1974) 513
- [6] SHAFRANOV, V.D., *On magnetohydrodynamical equilibrium configurations*, Sov. Phys. JETP., Vol. 6 (33), Number 3 (1958) 545
- [7] GOEDBLOED, J.P.: *Some remarks on computing axisymmetric equilibria*, Computer Phys. Commun., **2&3** (1984) 123
- [8] VAN MILLIGEN, B.Ph., *Exact relations between multipole moments of the flux and moments of the toroidal current density in tokamaks*, Nucl. Fusion **30** (1990) 157
- [9] VAN MILLIGEN, B. PH., SOLTWISCH, H., LOPES CARDOZO, N.J., *Application of Function Parametrization to the Analysis of Polarimetry and Interferometry data at TEXTOR*, submitted for publication in Nuclear Fusion (1990)

Figures

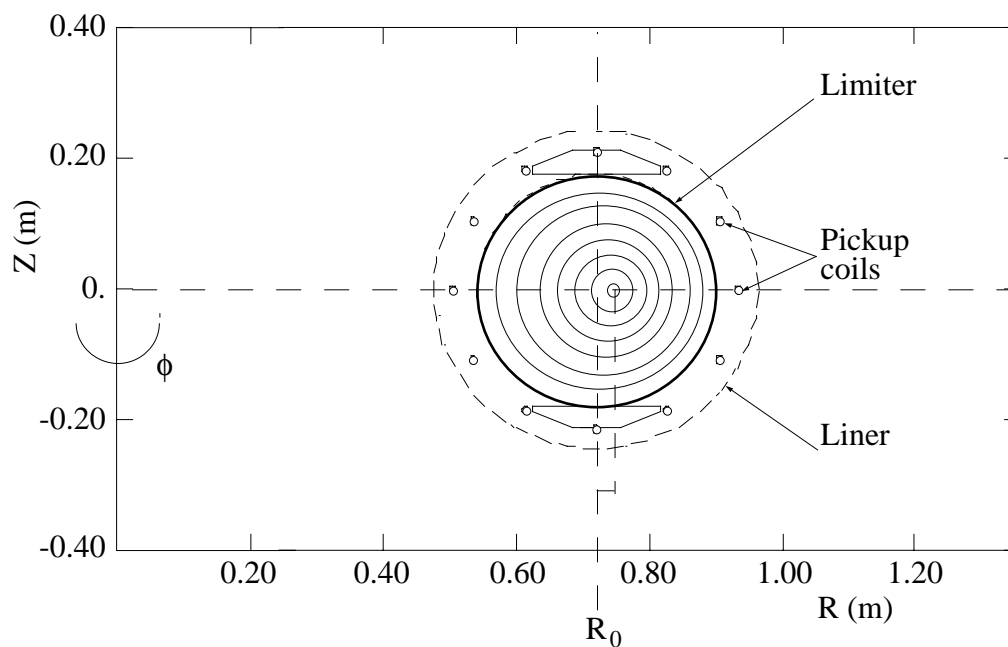


Fig. 3.1 Poloidal cross-section of the RTP Tokamak (to scale). The pickup-coils are shown and the radial field wire loops are attached to the liner. R_0 is the major radius of the tokamak (0.72 m). Also shown are examples of flux surfaces (solid circles). Δ is the shift of the magnetic axis.

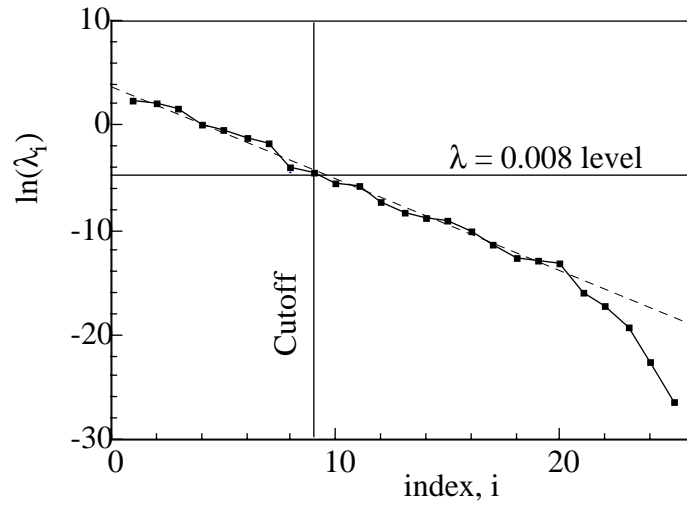


Fig. 3.2 Eigenvalues of the dispersion matrix of q versus the eigenvalue index number for the RTP database. The dashed line is the line $\ln(\lambda) = 3.68 - 0.878 i$. Also shown is the $\lambda = (3\epsilon)^2$ level which indicates that the eigenvalue cutoff should be placed at $i = 9$.

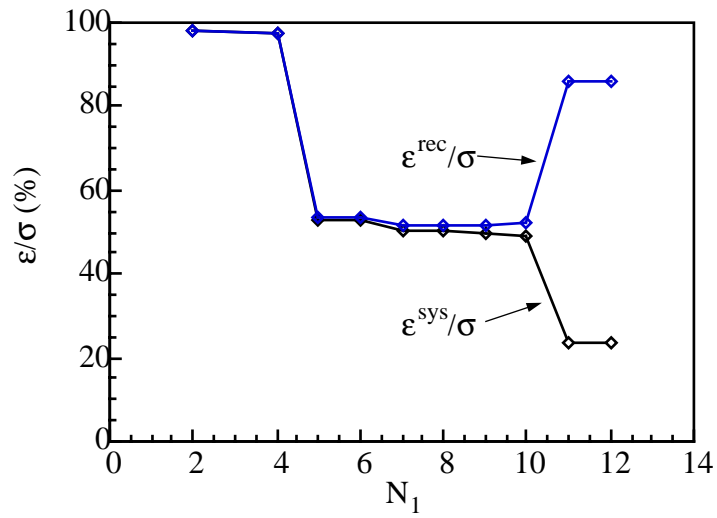


Fig. 3.3 Reconstruction error in a_{\min} as a function of N_1 . Shown are both the systematic error and the total (systematic and statistic) reconstruction error levels.

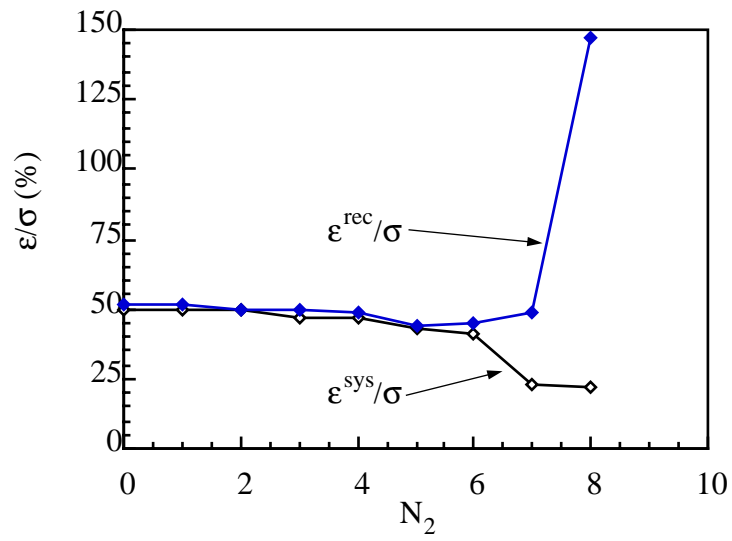


Fig. 3.4 Reconstruction error in a_{\min} as a function of N_2 with $N_1 = 8$. Shown are both the systematic error and the total (systematic and statistic) reconstruction error levels.

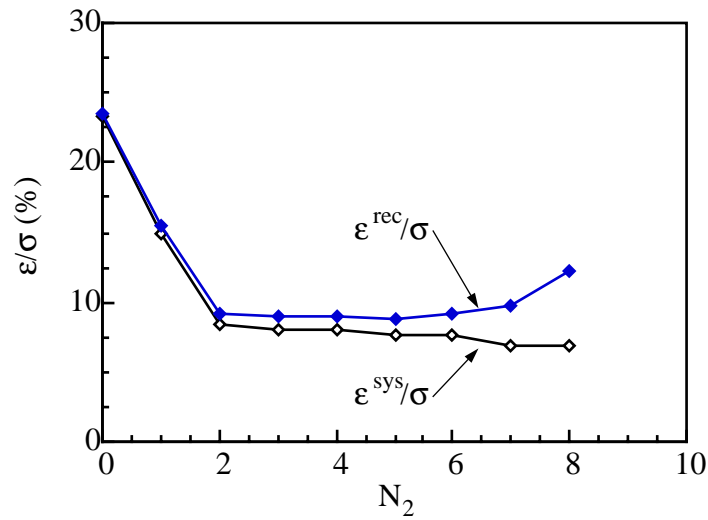


Fig. 3.5 Reconstruction error in R_{geo} as a function of N_2 with $N_1 = 8$. Shown are both the systematic error and the total (systematic and statistic) reconstruction error levels.

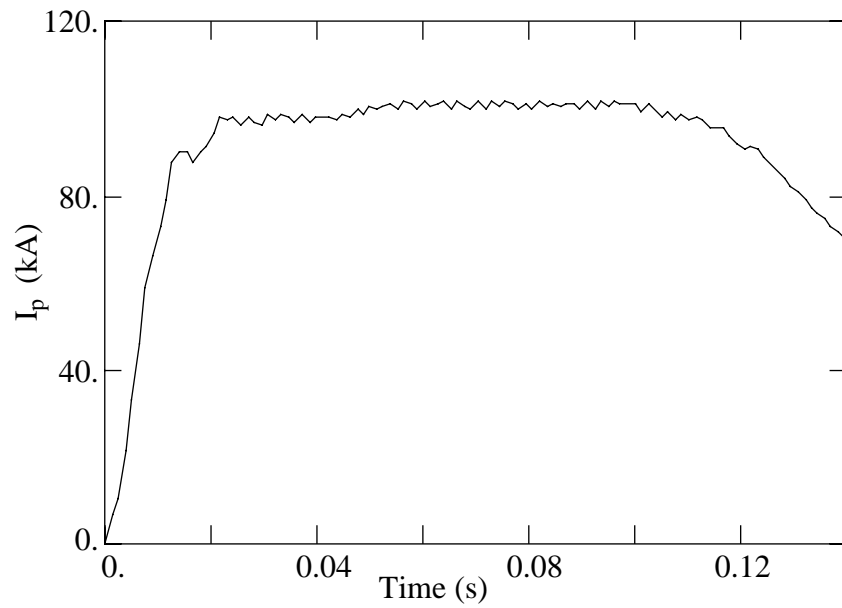


Fig. 3.6 Plasma current for discharge R19900321.017.

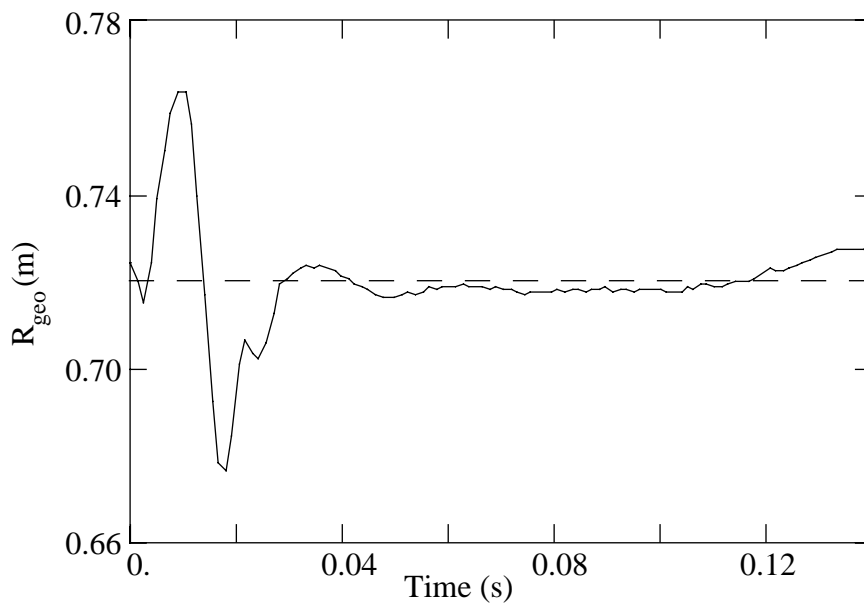


Fig. 3.7a Horizontal plasma position (FP) for discharge R19900321.017.

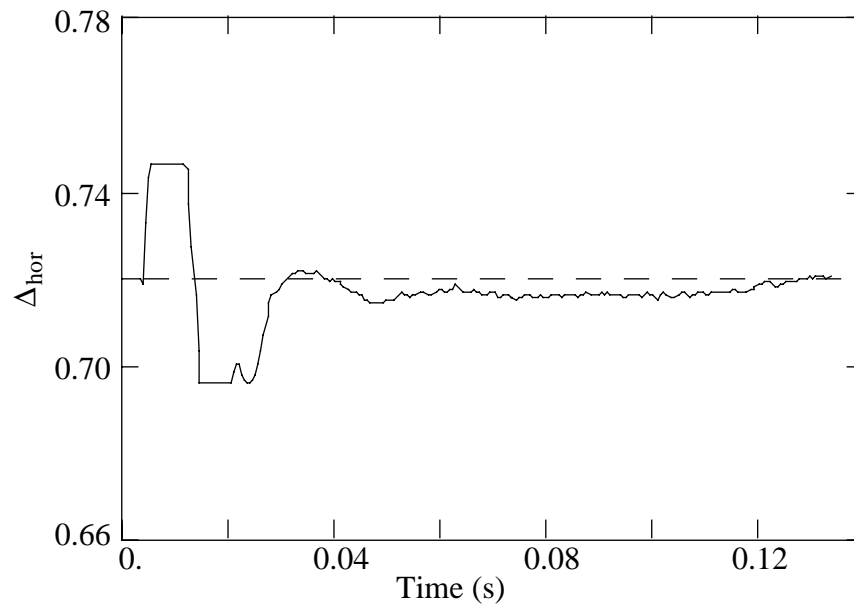


Fig. 3.7b Horizontal plasma position (traditional method) for discharge R19900321.017. The signal is computed by subtracting the inner and outer pickup-coil signals. Note that for $t < 0.03$ s the ADC signal exhibits saturation.

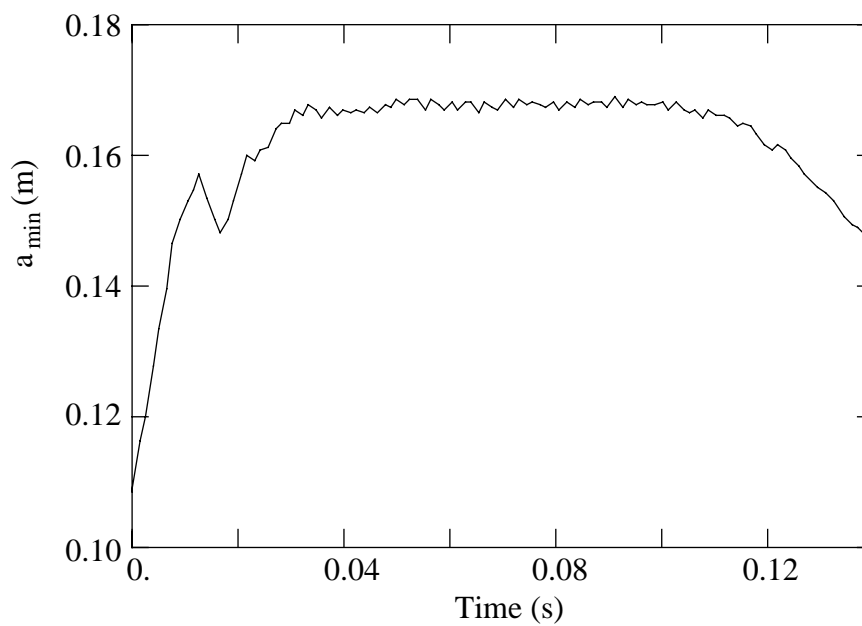


Fig. 3.8 Minor radius of plasma for discharge R19900321.017.

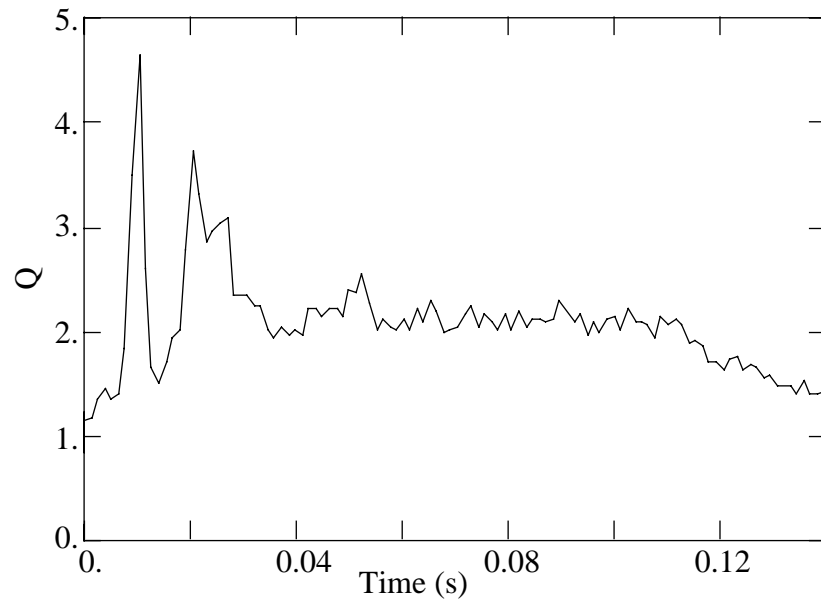


Fig. 3.9 Reconstruction qualifier Q for discharge R19900321.017.

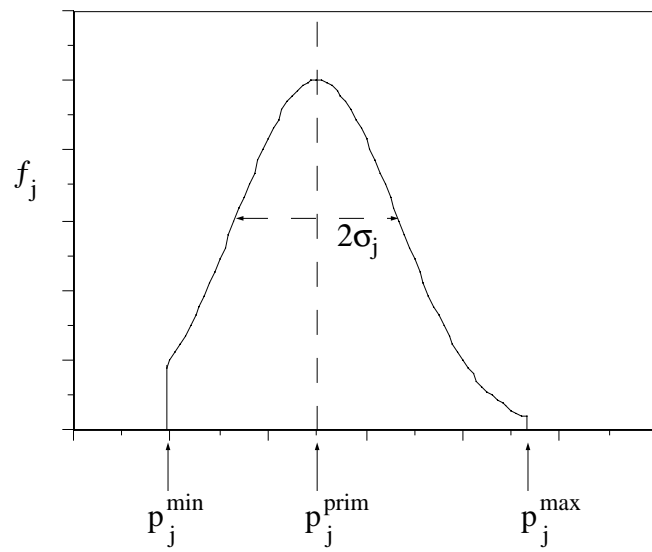


Fig. A.1 Truncated Gaussian probability distribution function.